Bull Earthquake Eng
DOI 10.1007/s10518-010-9199-1

ORIGINAL RESEARCH PAPER

# Comparison between non-linear dynamic and static seismic analysis of structures according to European and US provisions

**Mehmed Causevic · Sasa Mitrovic**

Received: 19 March 2010 / Accepted: 8 July 2010


**Abstract** Several procedures for non-linear static and dynamic analysis of structures have been developed in recent years. This paper discusses those procedures that have been implemented into the latest European and US seismic provisions: non-linear dynamic time-history analysis; N2 non-linear static method (Eurocode 8); non-linear static procedure NSP (FEMA 356) and improved capacity spectrum method CSM (FEMA 440). The presented methods differ in respect to accuracy, simplicity, transparency and clarity of theoretical background. Non-linear static procedures were developed with the aim of overcoming the insufficiency and limitations of linear methods, whilst at the same time maintaining a relatively simple application. All procedures incorporate performance-based concepts paying more attention to damage control. Application of the presented procedures is illustrated by means of an example of an eight-storey reinforced concrete frame building. The results obtained by non-linear dynamic time-history analysis and non-linear static procedures are compared. It is concluded that these non-linear static procedures are sustainable for application. Additionally, this paper discusses a recommendation in the Eurocode 8/1 that the capacity curve should be determined by pushover analysis for values of the control displacement ranging between zero and 150% of the target displacement. Maximum top displacement of the analyzed structure obtained by using dynamic method with real time-history records corresponds to 145% of the target displacement obtained using the non-linear static N2 procedure.

**Keywords** Non-linear dynamic analysis · Non-linear static methods · Pushover analysis · N2, NSP and CSM methods

M. Causevic (✉)
Faculty of Civil Engineering, University of Rijeka, V. C. Emina 5, Rijeka 51000, Croatia
e-mail: mehmed.causevic@gradri.hr

S. Mitrovic
Stabilnost, Rijeka, M. Albaharija 10a, Rijeka 51000, Croatia
e-mail: sasa.mitrovic@stabilnost.hr

Published online: 22 July 2010

## 1 Introduction

In the past few years, new methods of seismic analysis containing performance-based engineering concepts have been more frequently applied in order to pay greater attention to damage control. For obtaining seismic actions more realistically the displacement-based approach has proven itself as a much better choice than the traditional force-based approach.

The most precise description of the problem is by far the non-linear dynamic seismic analysis, made by applying time-history records which, in the long term, represents the correct development path. Yet, due to its complexity and high standards it goes beyond the frames of practical application and is appropriate only for the research and analysis of structures of special significance.

Between the linear methods and non-linear dynamic analysis, a non-linear static approach based on pushover analysis is being imposed as a link and the most economic solution at the moment. Thus, in recent years, the N2 method (Fajfar 2000) was implemented in European regulations (Eurocode 2004; Causevic and Zehentner 2007; Mitrovic and Causevic 2009; Rozman and Fajfar 2009). The Capacity Spectrum Method CSM and the coefficient method, that is the NSP (Non-linear Static Procedure), were introduced in US provisions (FEMA 1997, 2000 and 2005).

This paper presents the non-linear static methods which are an integral part of contemporary European and US provisions. These methods include the dynamic analysis of an equivalent SDOF (Single Degree Of Freedom) model. All the methods are presented in this paper using the example of the reinforced concrete frame structure (Fig. 1) and the obtained results are compared to the "accurate" results reached by a non-linear time-history analysis. The analyzed methods differ in simplicity of their application, and transparency and clarity of theoretical base, as well as the accuracy of the results. In each method, the determination of the target displacement is based on an explicitly-or implicitly-defined equivalent system with SDOF.

The pushover analysis is here performed in a way that the structure is subjected to a monotonously rising lateral load which represents the inertia forces which occur as a result of ground acceleration. By gradual increase of lateral load, a progressive yielding of structural elements occurs which results in reduction of stiffness of structure. The pushover analysis provides a characteristic non-linear curve of force-displacement relation and is most frequently presented as a relation of the total base shear $V$ and the top displacement $D_t$. This kind of presentation simultaneously provides data about load-bearing capacity, ductility and stiffness of the structure.

An important step in implementing the pushover analysis is determination of the appropriate distribution of the lateral load. The base assumption of the pushover analysis is the invariable form of displacement through time, which is reasonably accurate for linear response of structures vibrating dominantly in the first mode. However, in a non-linear field, the displacement form in reality is changing according to the dynamic characteristics change of the structure due to stiffness degradation, i.e. the formation of the plastic hinges.

## 2 Description of the building and the loading and the mathematical model

Application of all non-linear static and dynamic procedures is illustrated here by means of an example of an eight-storey reinforced concrete frame building. The first two storeys are 5.00 m high and the other 3.10 m (Fig. 1). All the columns have dimensions $60 \times 60$ cm with steel reinforcement equal for all cross sections. The beams have dimensions $40 \times 60$ cm,

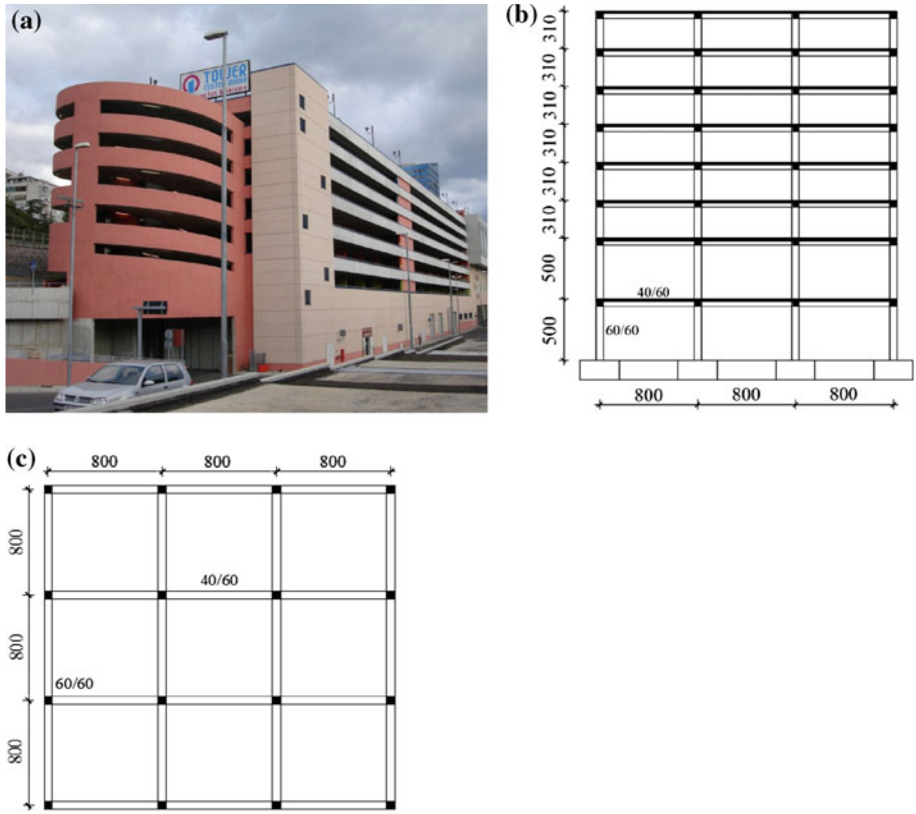


**Fig. 1** **a** Building of garage of the Tower Centre, Rijeka, Croatia; **b** Cross-section and **c** plan of one segment of the garage structure

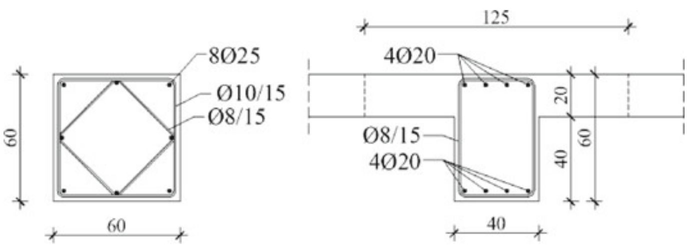


**Fig. 2** Cross-sections of columns and beams with steel reinforcement

also with steel reinforcement equal for all cross sections (Fig. 2). The plate is 20 cm thick. The concrete is of C25/30 class and the steel reinforcement is B500. Storey frame masses for 3.10 m high storeys are 67 t and storey masses for 5.00 m high storeys are 73.8 t which results in the mass total of 549 t.

The structure was designed according to the European standard (Eurocode 2004) with the following parameters: ground type B, importance class II ($\gamma_I = 1$), Type 1 elastic response spectra (the expected surface-wave magnitude $M_s$ larger than 5.5) and viscous damping ratio (in percent) $\xi = 5\%$. The analysis will be performed for the reference peak ground

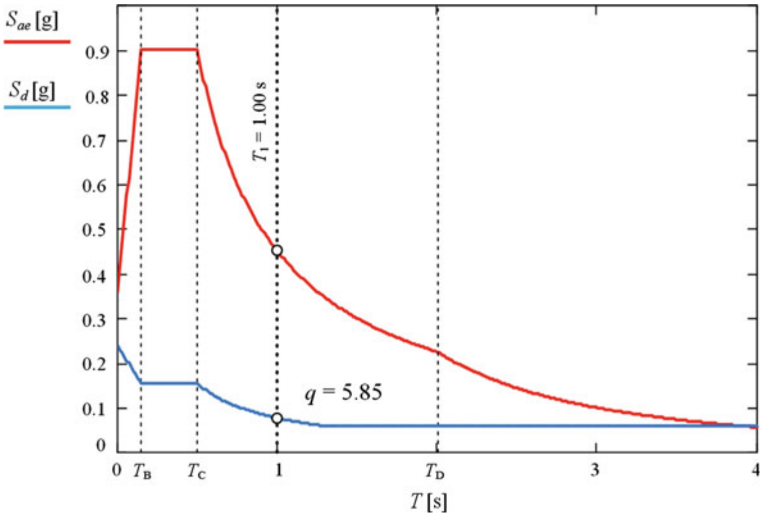


**Fig. 3** Elastic acceleration response spectrum with 5% viscous damping ratio for peak ground acceleration 0.3$g$, ground type B and corresponding design spectrum for behaviour factor 5.85

acceleration $a_{gR} = 0.3\,\text{g}$. A behaviour factor of $q = 5.85$ was taken into account for the DCH (Ductility Class High) structures.

Since the structure meets the regularity requirements by its plan view and by its height (Eurocode 2004), the current analysis was made on one plane frame. Due to symmetry only one direction of seismic action was analyzed and the fundamental period $T_1 = 1\,\text{s}$ for plane frame is obtained. According to the previously described parameters, the elastic acceleration response spectrum and the corresponding design spectrum are presented in Fig. 3 which represents the seismic demand. The fundamental period is in the spectrum range with constant velocities ($T_C < T_1 < T_D$).

The pushover and time-history analyses were performed by using the *SeismoStruct* program (Pinho 2007). Large displacements and rotations and P-Δ effect are taken into account through the employment of a total co-rotational formulation. Material inelasticity and the cross-section behaviour are represented through the so-called fibre approach where each fibre is associated with a uniaxial stress-strain relationship. A typical reinforced concrete section consists of unconfined concrete fibres, confined concrete fibres and steel fibres. A non-linear constant confinement concrete model and bilinear steel model with kinematic strain hardening are used. An incremental iterative algorithm with the employment of Newton-Raphson procedures is used to obtain the solution. The dynamic time-history analysis is computed by direct integration of the equations of motion with the Newmark scheme.

## 3 Non-linear time-history analysis

In order to evaluate the results obtained by non-linear static methods, a time-history dynamic analysis was conducted first by using a total of 14 time-history records, seven of which were artificial, and the remaining seven recorded (real). The artificial time-history records were used for obtaining the mean value of structural responses which corresponds to the specified seismic demand, while the real records were used for access to response variability.

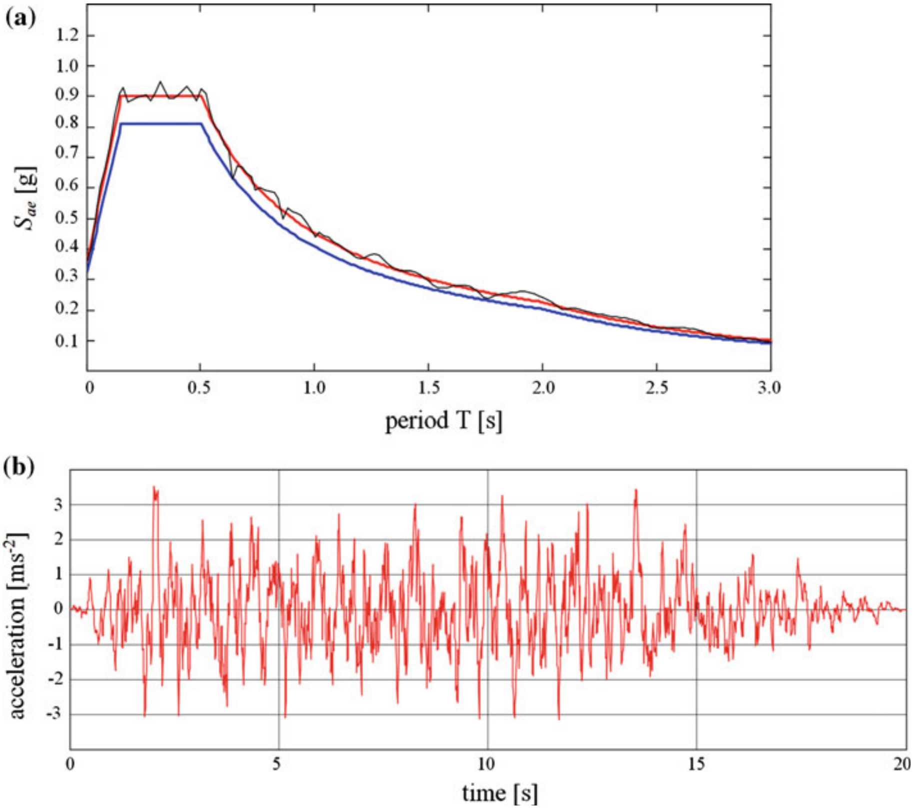


**Fig. 4** **a** Response spectrum with 5% viscous damping ratio for $a_g = 0.3g$ and soil class B (in *red*), its 90% value (in *blue*) and the response spectrum for the artificial time-history record no. 1 (in *black*); **b** the corresponding artificial digitalized time-history record no. 1

Processing of artificial and real time-history records was performed by using the *SeismoSignal* program (Pinho 2007).

Seven artificial time-history records for this example were generated by the program *SIMQKE_GR* (*SIMulation of earthQuaKE GRound motions—Massachusetts Institute of Technology*) (Gelfi 2007) for peak ground acceleration of $0.3g$ and soil class B with a 5% viscous damping ratio. The earthquake duration was set on 20 s. The acceleration value for zero period was set on $S \cdot a_g$ (according to Eurocode 8/1 $S$ is the soil factor, $a_g$ is the design ground acceleration on type A ground). In the zone near the fundamental period there is no value of elastic spectrum which is calculated from all time-history records, which is less than 90% of the corresponding value of the elastic spectrum response (Fig. 4). The zone near the fundamental period is defined (Eurocode 2004) within the limits between $0.2T_1$ (thus taking into consideration higher vibration modes) and $2T_1$ (thus taking into consideration the structural stiffness degradation due to earthquake and increase of the fundamental period as a consequence).

The real time-history records were taken from the libraries *National Information Service for Earthquake Engineering*, Berkeley, California and *The Canadian Association for Earthquake Engineering* (CAEE) (Naumoski 1988). All the selected time-history records were registered on the soil class A or B. The ratio of the maximum velocity to maximum acceleration ($v_{max}/a_{max}$) for all the selected records lies within the interval from 83 to 125, which corresponds to earthquakes of medium intensity (Naumoski et al. 1988). The following records were selected, Fig. 5a:

- Imperial Valley, California, USA (May 18th, 1940, El Centro);
- Ulcinj, Montenegro (April 15th, 1979, Hotel Albatros, Ulcinj);
- Mexico City, Mexico (September 19th, 1985, La Villita, Guerrero Array);
- Kocaeli, Turkey (August 17th, 1999, Sakaria);
- San Fernando, California, USA (February 9th 1971, 3838 Lankershim Blvd., L.A.);
- Honshu, close to the east coast, Japan (August 2nd, 1971, Kushiro Central Wharf);
- Kern County, California, USA (July 21st, 1951, Taft Lincoln School Tunnel).

The records were scaled according to Eurocode 8/1. It can be noted that for all selected records the acceleration value for zero period was set at $S \cdot a_g$ and accelerations for the fundamental period of the structure roughly coincide with the elastic acceleration response spectrum, Fig. 5a. The mean value of the scaled records represents well the elastic acceleration response spectrum, Fig. 5b.

Figure 6 presents the results obtained by using artificial records and Fig. 7 shows the results of using real records.

The mean value of responses obtained by real records corresponds to the mean value of responses obtained by artificial records. However, a considerably larger number of real records are required for obtaining the same accuracy.

## 4 The N2 method

The N2 method combines the pushover method of model with several degrees of freedom with a spectral analysis of the equivalent system with one degree of freedom, hence the name. The letter N states that it is a non-linear analysis and the number 2 states that two mathematical models are applied (Fajfar 2000). The method uses a non-linear spectrum in the format *acceleration–displacement*: AD. The format AD enables the simultaneous view of seismic demand and structural capacity. Intersection of seismic demand and structural capacity curves represents the required target displacement. The AD format is also used in the capacity spectrum method (CSM).

The main assumptions in the N2 method are: 1) its application to the structures which have no significant contribution of higher vibration modes; 2) the predominant mode does not change when the seismic intensity is changed (due to the formation of plastic hinges).

Listed assumptions apply also to the other methods according to US provisions which are discussed later in the text.

The acceleration spectrum which represents the seismic demand is plotted in Fig. 3.

In case of the analyzed structure, Fig. 1, the mass matrix is the diagonal $8 \times 8$ matrix with diagonal elements equal to the storey masses.

The influence of the proposed three kinds of shape on the overall results for the N2 method is presented firstly. The assumed shapes are:

$$\Phi^{\mathrm{T}} = [1.00\ 1.00\ 1.00\ 1.00\ 1.00\ 1.00\ 1.00\ 1.00] \quad \text{uniform}$$
$$\Phi^{\mathrm{T}} = [0.17\ 0.35\ 0.46\ 0.57\ 0.67\ 0.78\ 0.89\ 1.00] \quad \text{triangular}$$
$$\Phi^{\mathrm{T}} = [0.24\ 0.56\ 0.69\ 0.79\ 0.87\ 0.93\ 0.97\ 1.00] \quad \text{modal}$$

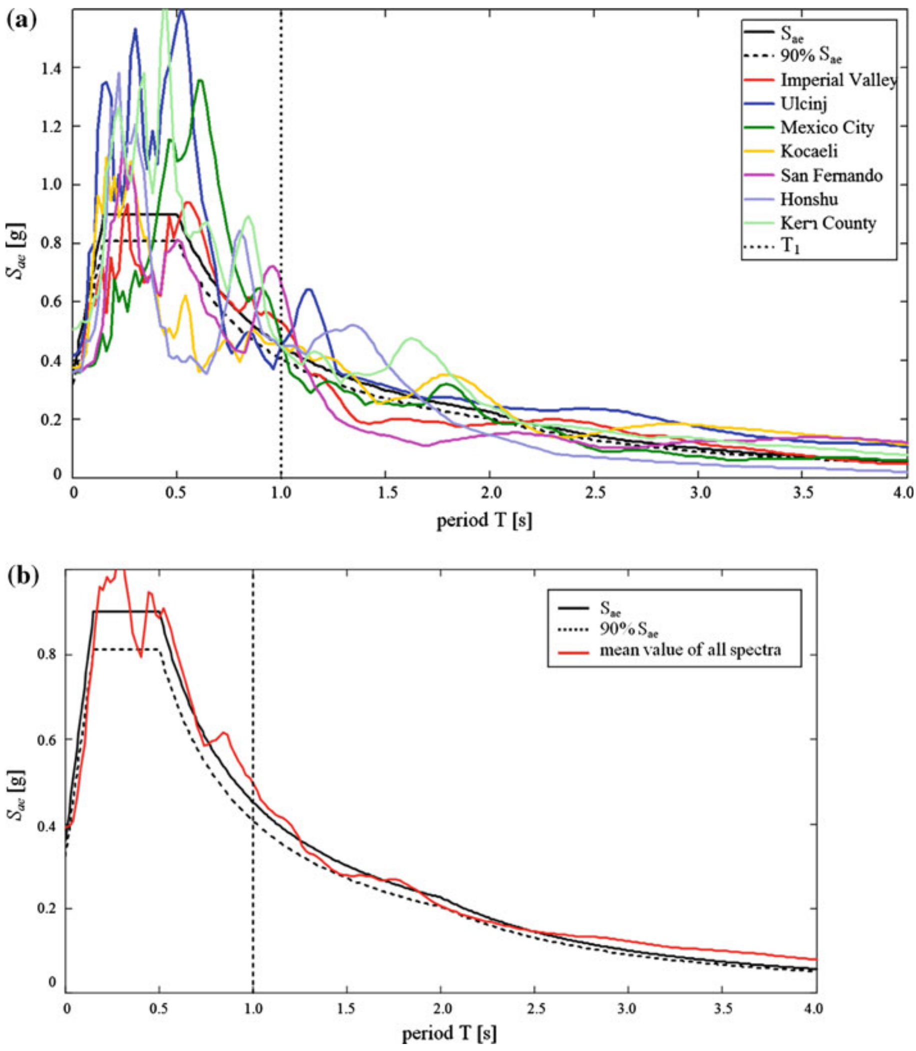


**Fig. 5** **a** Acceleration response spectrum of the selected real earthquakes together with the required response spectrum and its 90% value; **b** mean value of all spectra

The distribution of lateral forces is normalized by assigning the roof force the unit value:

$$P^T = [1.10\ 1.10\ 1.00\ 1.00\ 1.00\ 1.00\ 1.00\ 1.00] \quad \text{uniform}$$
$$P^T = [0.15\ 0.31\ 0.41\ 0.51\ 0.60\ 0.70\ 0.89\ 1.00] \quad \text{triangular}$$
$$P^T = [0.26\ 0.62\ 0.69\ 0.79\ 0.87\ 0.93\ 0.97\ 1.00] \quad \text{modal}$$

Figure 8 presents the capacity curves for this structure for the different shapes (uniform, triangular, modal).

Figure 9 presents the capacity curve for the assumed triangular shape and its bilinear idealization. The capacity curve is idealized by elastic-perfectly plastic force-displacement relation. For determining the yielding limits an engineering judgment is required. If the

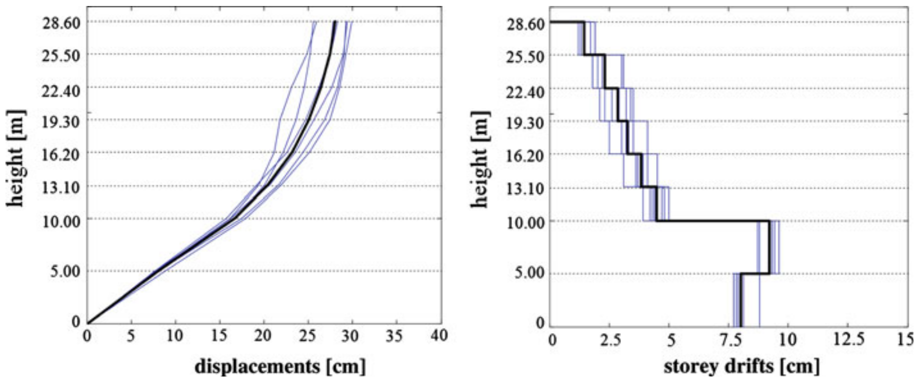


**Fig. 6** Displacements and storey drifts for structure in Fig. 1 for all seven artificial time-history records (in *blue*) and their mean value (in *black*)

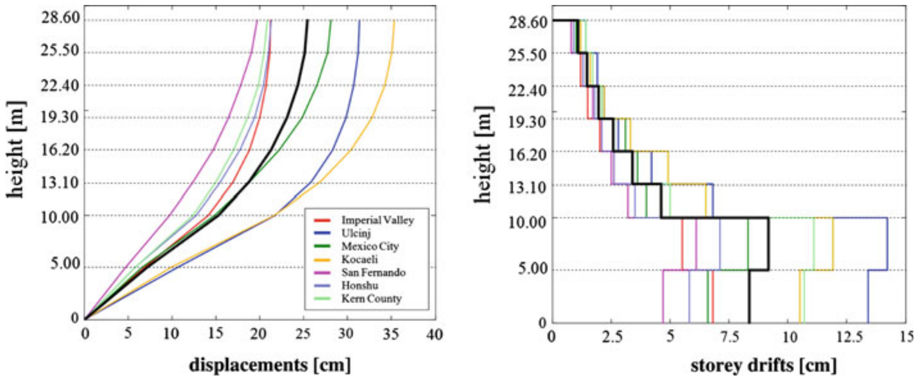


**Fig. 7** Displacements and storey drifts for structure in Fig. 1 for all 7 real time-history records and their mean value (in *black*)

approach of equal energies is used, the larger adopted yielding limit value means also the lesser initial stiffness and vice versa. The yielding limit can be adopted at the beginning of a plastic mechanism occurrence. This generally enables a more conservative estimation of seismic demand and lesser initial stiffness.

The transformation factor Γ is a well known modal participation factor which controls the transformation from MDOF to the SDOF model and is defined as

$$\Gamma = \frac{\Phi^{\mathrm{T}}\mathrm{m}1}{\Phi^{\mathrm{T}}\mathrm{m}\Phi} = \frac{\sum m_i \Phi_i}{\sum m_i \Phi_i^2} = \frac{m^*}{\sum m_i \Phi_i^2} \tag{1}$$

Note that the same transformation factor Γ is valid for both the displacement transformation and force transformation. As a consequence, the force–displacement relation is the same for both systems and differs only in scaling factor Γ. Both systems have also the same initial stiffness. The equivalent mass $m^*$ and transformation factor Γ for the triangular form have the following values:

$$m^* = 331.10\,\mathrm{t}$$
$$\Gamma = 1.39$$

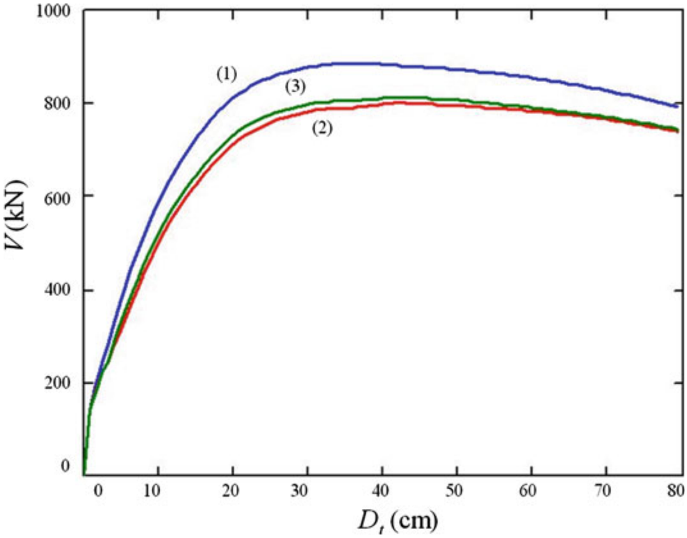


**Fig. 8** Pushover *curve* for three different shapes: the uniform (*1*), the triangular (*2*) and the modal (*3*)

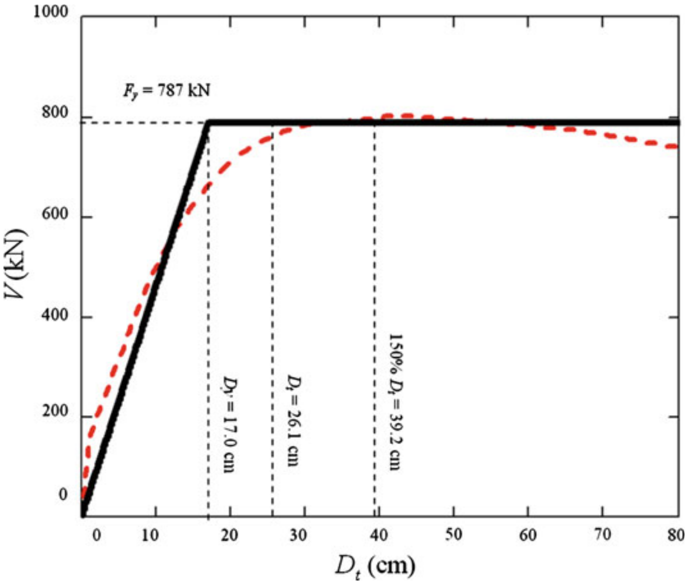


**Fig. 9** Capacity *curve* for the assumed triangular shape (the *dotted line* for the real capacity *curve* and the *solid line* for the elasto-plastic idealization)

For uniform and modal shape the transformation factor Γ amounts to 1.00 and 1.21, respectively.

The elastic period of the idealized elasto-plastic system can be determined as:

$$T^* = 2\pi\sqrt{\frac{m^* D_y^*}{F_y^*}} \tag{2}$$

where $F_y^*$ and $D_y^*$ are the yield strength and displacement, respectively, for equivalent SDOF system.

From the elasto-plastic capacity curve shown in Fig. 9 the values $F_y$ and $D_y$ can be taken. Knowing constant $\Gamma$ the corresponding values for SDOF system can be obtained.

$$F_y^* = \frac{F_y}{\Gamma} = 565.86\,\text{kN}$$
$$D_y^* = \frac{D_y}{\Gamma} = 12.22\,\text{cm}$$

The elastic period of equivalent SDOF system has the value:

$$T^* = 2\pi\sqrt{\frac{m^* D_y^*}{F_y^*}} = 1.68\,\text{s}$$

Finally, the capacity diagram in AD format can be obtained by dividing the forces in the force–deformation diagram ($F^*\!-\!D^*$) by the equivalent mass $m^*$:

$$S_a = \frac{F^*}{m^*} \tag{3}$$

The acceleration on the yielding limit has the following value, Fig. 10:

$$S_{ay} = \frac{F_y^*}{m^*} = 0.17g$$

The solution can be determined both graphically and analytically (Fig. 10). The section point of the radial straight line which corresponds to the elastic period $T^*$ of the ideal bilinear system with elastic demand spectrum determines the acceleration demand $S_{ae}$ required for the elastic behaviour and the corresponding elastic displacement demand $S_{de}$. The acceleration at the yielding limit also represents the acceleration demand and capacity of the inelastic system. The reduction factor $R_\mu$ is determined as a ratio of accelerations which correspond to the elastic and the inelastic system:

$$R_\mu = \frac{S_{ae}(T^*)}{S_{ay}} = \frac{0.268\text{g}}{0.174\text{g}} = 1.54 \tag{4}$$

The inelastic displacement demand $S_d$ is identical to the elastic displacement demand $S_{de}$ (identical displacement rule) while the demanded ductility $\mu$ is identical to the reduction factor $R_\mu$.

$$S_d = S_{de}(T^*) \tag{5}$$
$$\mu = R_\mu = 1.54 \tag{6}$$

Figure 10 presents the elastic spectrum, the demand spectrum and the capacity diagram in AD format.

The inelastic demand is represented by the section point of the capacity diagram with the demand spectrum which corresponds to the required ductility $\mu$, Fig. 10.

The displacement demand of the equivalent SDOF system is transformed back to the target displacement of the MDOF system. The maximum displacements of stories are represented by an envelope of results obtained by calculations with different assumed shapes. The target displacements for ground acceleration of 0.3$g$ have the following values:

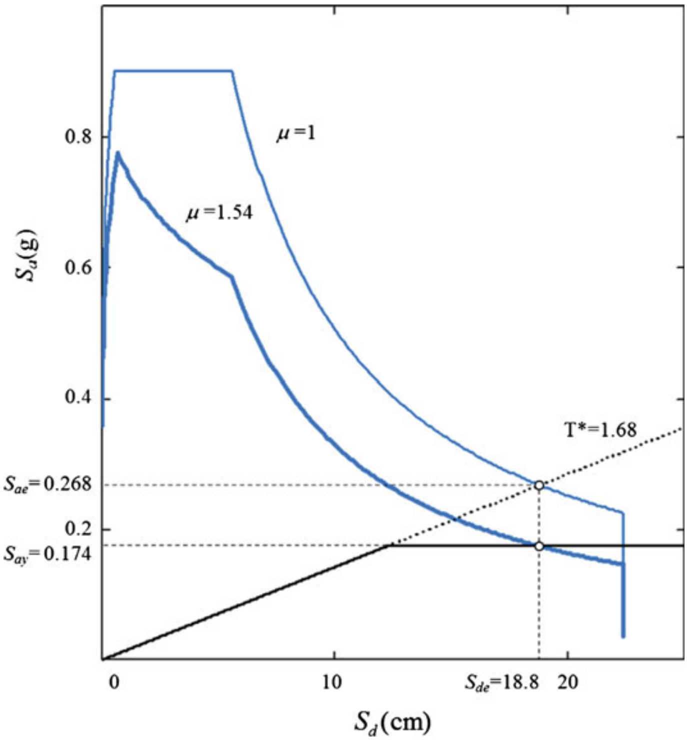


**Fig. 10** The demand spectrum for ground acceleration 0.3$g$ (soil class B) and capacity spectrum for the garage structure in Fig. 1b

$$D_t = 1.00 \cdot 22.1\,\text{cm} = 22.1\,\text{cm} \quad \text{uniform}$$
$$D_t = 1.39 \cdot 18.8\,\text{cm} = 26.1\,\text{cm} \quad \text{triangular}$$
$$D_t = 1.21 \cdot 20.7\,\text{cm} = 25.1\,\text{cm} \quad \text{modal}$$

Under monotonically increasing lateral loads the structure is pushed to its top displacement $D_t$ (pushover analysis), which provides displacements as the global seismic demand and storey drifts, joint rotations, etc., as the local seismic demands for the whole structure. Figures 11 and 12 present the storey displacements and the storey drifts for all three assumed shapes.

The analysis of the structural damage is performed by comparing the seismic demand with the capacities of corresponding performance levels. Deformation of the structure corresponding to 150% of target displacement and the rotations in the elements for the analyzed structure are shown on Figs. 13 and 14.

## 5 The non-linear static procedure (NSP)

Target displacement $\delta_t$ in the NSP is determined by the coefficient method (FEMA 2000) in the following way:

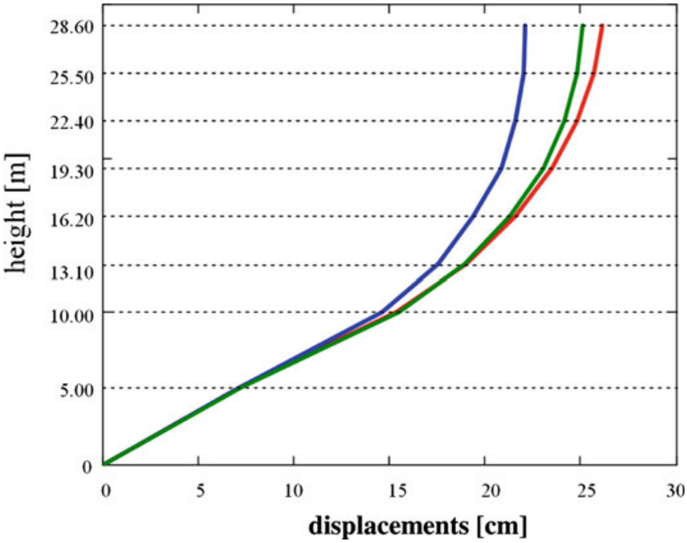


**Fig. 11** Displacements for three assumed shapes: uniform (in *blue*), triangular (in *red*) and modal (in *green*) storey drifts (cm)

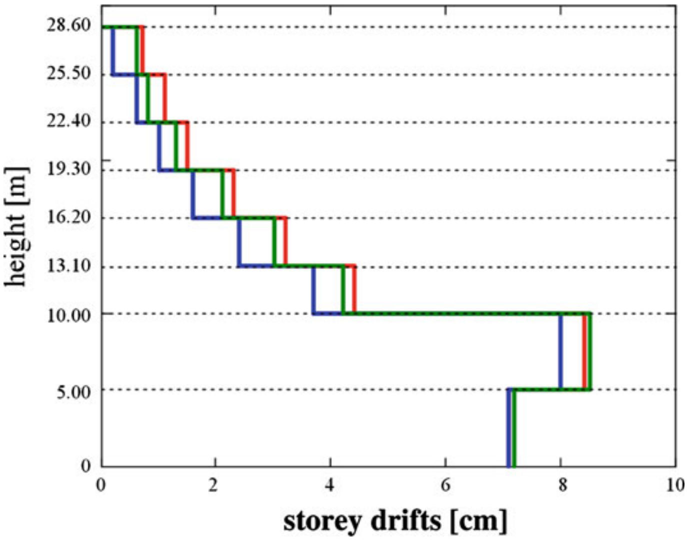


**Fig. 12** Storey drifts for three assumed shapes: uniform (in *blue*), triangular (in *red*) and modal (in *green*)

$$\delta_t = C_0 C_1 C_2 C_3 S_a \frac{T_e^2}{4\pi^2} g \tag{7}$$

$T_e$ is the effective period of the structure;

$S_a$ is the value of the acceleration response spectrum for the effective fundamental period of the structure for the required direction expressed as a part of the gravity acceleration $g$.

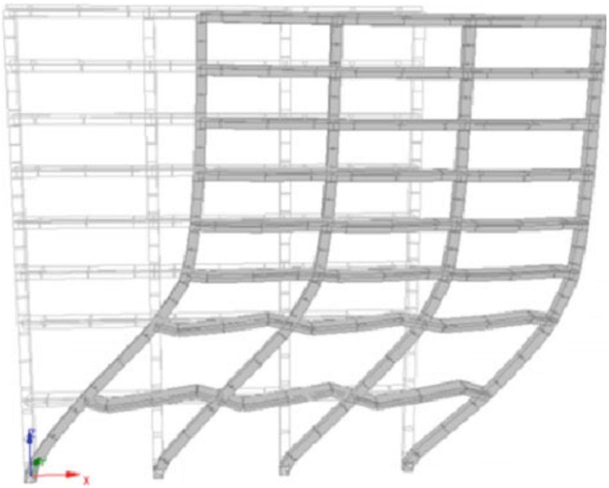


**Fig. 13** Deformation of the structure corresponding to 150% of target displacement

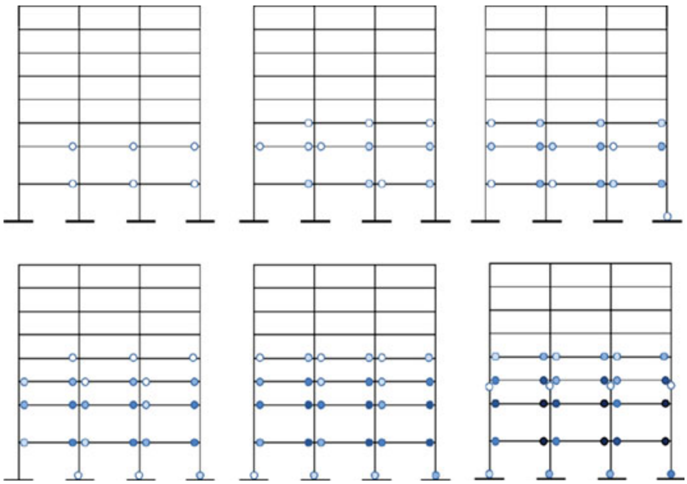

**Fig. 14** Rotations in the elements presented in steps of 0.2%. Rotations are proportional to the intensity of *darkness of the mark*. The maximum rotation amounts to 1%

The value of the target displacement, the effective period and the idealization of the push-over curve are mutually dependable. Therefore an iteration procedure must be conducted in order to obtain the final solution. The coefficient values $C_0$, $C_1$,... are shown in tables (FEMA 2005).

The non-linear relation between the total base shear and roof displacement is idealized with a bilinear relation, according to which the effective stiffness of the structure $K_e$ and the yielding limit force $V_y$ are determined. The effective lateral stiffness of the structure is presumed to be the secant stiffness, which is determined by the shear force at 60% of the maximum shear force.

The effective period and the target displacement (Fig. 15) have been calculated for the triangular lateral force distribution and value of modification factor $C_0$ taken from the table (FEMA 2005).

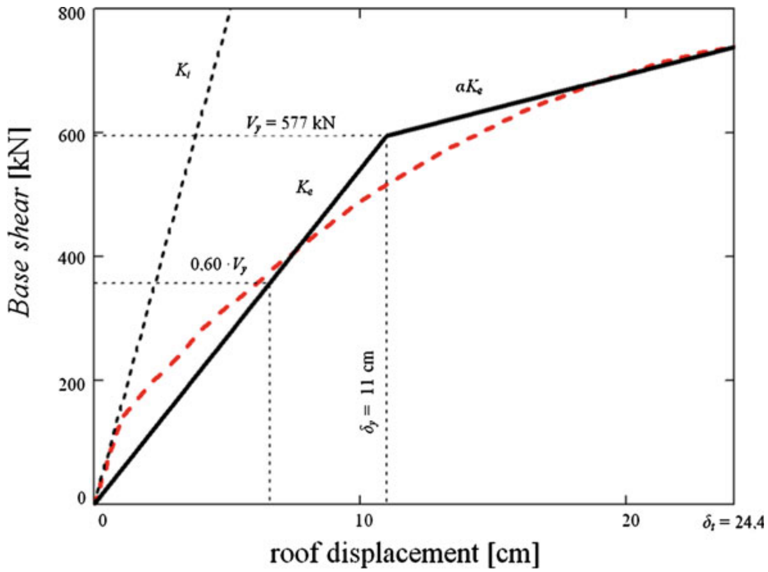


**Fig. 15** Bilinear idealization of pushover *curve* for the triangular lateral force distribution shape and $C_0 = 1.3$

$$T_e = T_i\sqrt{\frac{K_i}{K_e}} = 1.00s \cdot \sqrt{\frac{15600}{5529}} = 1.68s$$

$$\delta_t = C_0C_1C_2C_3S_a\frac{T_e^2}{4\pi^2}g = 1.3 \cdot 1.0 \cdot 1.0 \cdot 1.0 \cdot 0.268 \cdot \frac{(1.68s)^2}{4\pi^2}9.81\frac{m}{s^2} = 24.4\,\text{cm}$$

The bilinear idealization of the pushover curve was performed by equating the surfaces below the real and the idealized curve in the range between 0 and target displacement $\delta_t$.

If the exact value of the coefficient $C_0 = \Phi_{1i}\Gamma_i = 1.39$, $(\Phi_{1i} = 1)$ is used, the target displacement has the value 25.4 cm.

Displacements and storey drifts along the structure height obtained using the non-linear static procedure NSP have the same shape as in the N2 method (Figs. 11, 12) because the same pushover calculation with the same distribution shapes of lateral load is used.

## 6 The capacity spectrum method (CSM)

The main assumption of the capacity spectrum method (FEMA 2005) is that the maximum non-linear deformations of the system with one degree of freedom can be approximated by equivalent linear system deformations whose coefficient of the internal viscous damping is larger than the initial value of non-linear system damping. According to this assumption, when determining the earthquake demand, the equivalent linear spectrum defined by the equivalent damping $\xi_{eq}$ is used. The idealization of the pushover curve is based on secant stiffness in a similar way as in the previously described coefficient method. The bilinear idealization consists of an elastic line with the stiffness $k$ which, after having reached the yielding limit defined by $f_y$ and $u_y$, traverses into the line with stiffness $\alpha\, k$ (Fig. 16).

The equivalent viscous damping is obtained by equalizing the dissipated energy during one cycle of vibration of the non-linear system and the equivalent linear system. The equivalent

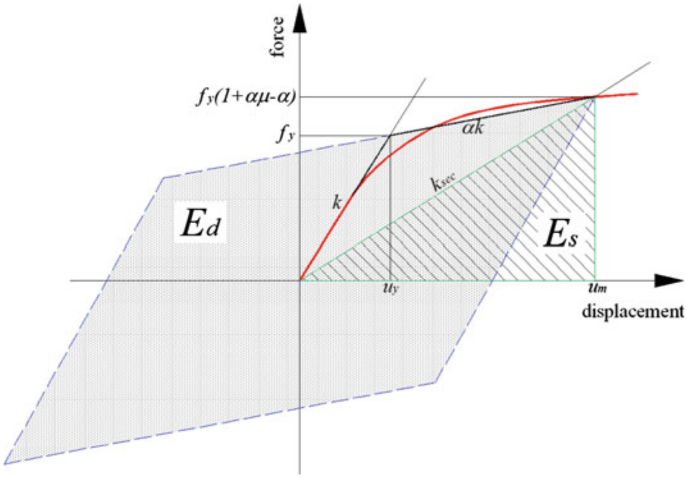


**Fig. 16** Nonlinear system with one degree of freedom, presentation of equivalent viscous damping based on hysteretic energy dissipation

viscous damping ratio is defined by the equation (Chopra and Goel 1999, 2002):

$$\xi_{eq} = \frac{1}{4\pi}\frac{E_D}{E_S} \tag{8}$$

where: $E_D$ is the energy dissipated in the non-linear system which equals the hysteresis loop surface (parallelogram in Fig. 16). $E_S$ is the energy dissipation of linear system which equals triangle surface $k_{sec}u_m/2$, whose stiffness is $k_{sec}$, Fig. 16.

From the expression (8) and Fig. 16 the equivalent viscous damping ratio can be determined:

$$\xi_{eq} = \frac{2}{\pi}\frac{(\mu-1)(1-\alpha)}{\mu(1+\alpha\mu-\alpha)} \tag{9}$$

The total viscous damping of the equivalent linear system is:

$$\hat{\xi}_{eq} = \xi_0 + \xi_{eq} \tag{10}$$

where $\xi_0$ is the viscous damping ratio of bilinear system for vibrations in linear range ($u \le u_y$).

## 6.1 Procedure according to ATC-40

Taking into consideration that the secant stiffness and the equivalent damping ratio depend on the target displacement, the iteration procedure in determining the maximum displacement is required. In ATC 40 three iteration procedures are described, two of which are analytical and one graphical. Chopra and Goel (1999, 2002) have shown that the procedures do not always converge and more than one solution is possible when real spectra are used. It has also been shown that the results obtained by this method, when compared to the results obtained by non-linear time-history analysis, differ up to 50%, which proves this method unreliable.

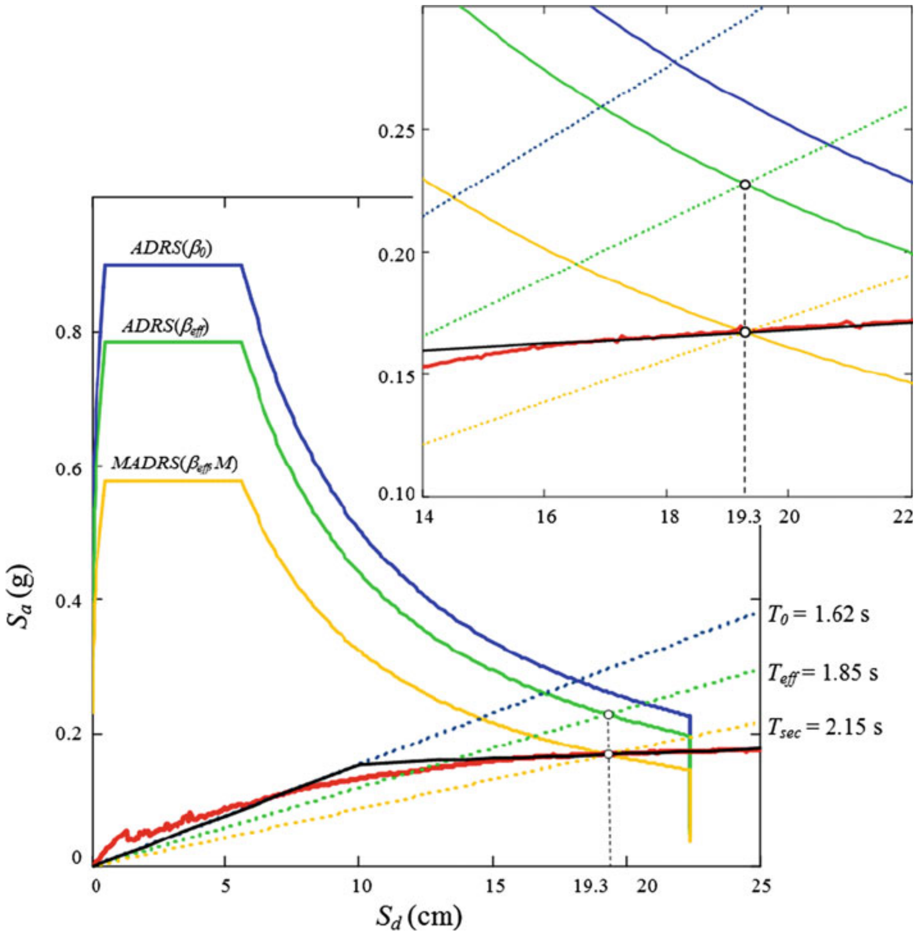


**Fig. 17** Graphical presentation of solution for the triangular distribution of lateral load

6.2 Improved procedure according to FEMA-440

The improved procedure (FEMA 2005) is also based on equivalent linearization, the equivalent values being determined by coefficients in correlation to the hysteretic performance and stiffness of the system after yielding. These coefficients are based on a large number of analyzed non-linear systems with one degree of freedom and are optimized so that they correspond to the empiric values.

New symbols are introduced: $\beta_{eff}$ for the total viscous damping and $\beta_0$ for the viscous damping ratio of the system for vibrations in the linear field and $T_{sec}$ for the equivalent period.

The target displacement is represented by intersection of the effective period and the response spectrum in AD format for the equivalent damping ADRS($\beta_{eff}$): Procedure A (direct iteration, Fig. 17). The same solution is provided by the intersection of the secant period with the modified response spectrum MADRS ($\beta_{eff}$, $M$): Procedure B (intersection with MADRS, Fig. 17). The reduction of the elastic spectrum with 5% viscous damping on the spectrum with the equivalent damping $\beta_{eff}$ is determined according to the following expression which defines ADRS($\beta_{eff}$) (the acceleration values of the diagram are reduced only):

$$S_{a\beta} = \frac{S_{a0}}{B(\beta_{eff})} \tag{11}$$

$S_{a\beta}$ is the elastic spectrum acceleration with viscous damping $\beta_{eff}$,
$S_{a0}$ is the elastic spectrum acceleration with 5% viscous damping,
B ($\beta_{eff}$) being the reduction factor which is: $4/(5,6 - \ln \beta_{eff})$.

The modified response spectrum MADRS ($\beta_{eff}$, $M$) is obtained by multiplying the ADRS ($\beta_{eff}$) values with the modification factor M (Fig. 17):

$$M = \frac{a_{max}}{a_{eff}} = \left(\frac{T_{eff}}{T_{sec}}\right)^2 \tag{12}$$

Figure 17 presents the results for the triangular lateral load distribution. The target displacement of the equivalent system with one degree of freedom is 19.3 cm and that of the original system is $1.39 \cdot 19.3 = 26.8$ cm (Fig. 17, Table 5).

## 7 Comparison of presented methods

The discussed non-linear static methods differ in their application simplicity, transparency and clarity of the theoretical basis. The basis of all methods is the same, i.e., the pushover method, while the main difference is the determination of the pushover limit of the target displacement. Both approximations and limitations of the non-linear static methods are connected to those two steps.

### 7.1 Particularities of methods

Table 1 offers a brief review of basic differences between the analyzed non-linear static methods. The following particularities have been analyzed:

- the type of used spectrum;
- the idealization of pushover curve and the need for the iteration procedure;
- the consistency of transformation of a SDOF system into the original system with MDOF;
- the possibility of graphical presentation.

### 7.2 The N2 method

In the presented formulation of the N2 method, the simplified non-linear spectrum, which is based on the equal displacement rule for structures with medium and long periods, is used.

**Table 1** Review of the basic characteristics of non-linear static methods

| Method | Spectrum type | Iteration requirement | Transformation consistency SDOF→MDOF | Graphical presentation |
|---|---|---|---|---|
| N2 | Non-linear | No | Yes | Yes |
| NSP | Non-linear | Yes | No | No |
| CSM | Equiv. linear | Yes | No | Yes |

The applicability of this rule has been confirmed by numerous statistical studies and it provides the best results for firm soils and structures with stabile and full hysteresis loops. In the N2 method, for its simplicity, the elastic-perfectly plastic relation between the force and the displacement was proposed. A moderate value of post-yield stiffness (related to coefficient $\alpha$) has no significant influence on the demanded displacement and the proposed inelastic spectrum is adequate for structure without strengthening or with little strengthening. The bilinear idealization depends, to some extent, on engineering judgment. In codes, however, the procedure should be clearly defined. The displacement demand depends on the equivalent stiffness which depends on the target displacement. In Eurocode 8, for performing the bilinear idealization based on the equal energy concept, the displacement corresponding to the formation of the plastic mechanism can be assumed as the target displacement. In such a case, there is no need for the iteration procedure. If the target displacement value is expected to be considerably less than the displacement at the formation of the plastic mechanism formation, an iteration procedure is, in principle, necessary. In the Annex B of EC8/1 an iterative procedure is recommended for such a case (see B.5 of EC8/1). The iterative procedure leads to a larger equivalent stiffness. To some extent, the idealization depends on engineering judgment.

### 7.3 The NSP method

The inelastic spectrum used in this method is identical to the inelastic spectrum used in the N2 method. The idealization of the pushover curve is required. It depends on the target displacement, which makes the procedure iterative. The pushover curve is idealized by a bilinear relation in which the value of stiffness, after having reached the yielding point, generally differs from zero. The positive value of stiffness after the yielding point ($\alpha > 0$, Fig. 16) has no influence on the target displacement. The effective stiffness is assumed to be identical to the secant stiffness which is determined by the shear force at the value of 60% of the force at the yielding limit.

The coefficient $C_0$, which connects the maximum displacement of the SDOF system and the maximum roof displacement of the original structure, is defined in the same way as transformation factor $\Gamma$ in the N2 method. However, the transformation of the SDOF system into the original system is theoretically inconsistent due to the allowed partial or complete independence of displacement and force forms. In this process the transparency and clarity are lost, yet no significant influence on accuracy occurs.

### 7.4 The CSM method

The capacity spectrum method uses the equivalent linear spectrum which is determined by the equivalent damping. The pseudo acceleration spectrum which determines the seismic demand is practically the same as the spectrum of the total acceleration for lower values of the damping. However, by increasing the damping, the difference between the pseudo acceleration and the total acceleration increases on the unsafe side. The error increases also with an increase of the fundamental period. Having in mind the theoretical basis for the equivalent linearization, the advantage of the inelastic spectra used in other two methods is obvious.

A bilinear idealization of the pushover curve is required. The value of the effective damping ratio depends on ductility and stiffness after yielding. In this method, the idealization also depends on the target displacement so the iteration procedure is required. The transformation of the SDOF system into the original system is identical to the one in N2 method. The graphical presentation is made in AD format. Both presented procedures for determining the target displacement can be graphically presented.

### 7.5 Comparison

It can be concluded that the N2 method and the NSP coefficient method are basically very similar and provide the same results if the starting assumptions are identical. In the NSP coefficient method there are two additional coefficients which influence the value of the target displacement and which are not included into the other two methods (N2 and CSM): the coefficient $C_2$ which represents the effects of stiffness and strength degradation for maximum structure displacements and the coefficient $C_3$ which represents the displacement increase due to the dynamic P-$\Delta$ effect. The influence of coefficients $C_2$ and $C_3$ can easily be included into two other methods (N2 and CSM) in a way that the target displacement is multiplied by the corresponding modification factor. The N2 and NSP methods yield identical results if $C_2 = 1$ and $C_3 = 1$ and if the same effective stiffness is used.

Neither of the analyzed methods takes into consideration the accumulation of the damage which can be significant for long duration earthquakes. The inclusion of this effect into existing methods can be made by increasing the seismic demand or by introducing the equivalent ductility factor like in the N2 method, which reduces the deformation capacity (Fajfar and Gaspersic 1996).

The comparison of the results obtained for the structure from Fig. 1 was performed. Tables 2 and 3 offer the comparative characteristic values of the used methods for the assumed triangular and uniform displacement forms.

The non-linear static coefficient method is represented by two sets of results: in one case the value of the coefficient $C_0$ was taken from the corresponding tables (designation NSP) while in the other case the accurate coefficient value $C_0$ was used (designation NSP*).

Taking into consideration that the non-linear time history analysis is the most accurate method, its results were used for evaluating other methods. The maximum target

**Table 2** Characteristic values for triangular displacement form

| Triangular displacement form | N2 | NSP | NSP* | CSM |
|---|---|---|---|---|
| $C_0$ or $\Gamma$ | 1.39 | 1.3 | 1.39 | 1.39 |
| $K_e$ (kN/m) | 4629 | 5529 | 5838 | 4980 |
| $\alpha$ | 0 | 0.19 | 0.19 | 0.09 |
| $T_{ef}$ or $T*$ (s) | 1.68 | 1.68 | 1.64 | 1.85 |
| $\delta_t$ or $D_t$ (cm) | 26.1 | 24.4 | 25.4 | 26.8 |

**Table 3** Characteristic values for uniform displacement form

| Uniform displacement form | N2 | NSP | NSP* | CSM |
|---|---|---|---|---|
| $C_0$ or $\Gamma$ | 1.0 | 1.2 | 1.0 | 1.0 |
| $K_e$ (kN/m) | 5526 | 7351 | 7325 | 5800 |
| $\alpha$ | 0 | 0.23 | 0.24 | 0.15 |
| $T_{ef}$ or $T*$ (s) | 1.98 | 1.46 | 1.64 | 1.84 |
| $\delta_t$ or $D_t$ (cm) | 22.1 | 19.5 | 16.3 | 25.0 |

**Table 4** Target displacement for different methods

| Method | N2 | NSP | NSP* | CSM | Time-history real | Time-history artificial |
|---|---|---|---|---|---|---|
| Maximum displ. (cm) | 26.1 | 24.4 | 25.4 | 26.8 | 27.7 | 28.0 |

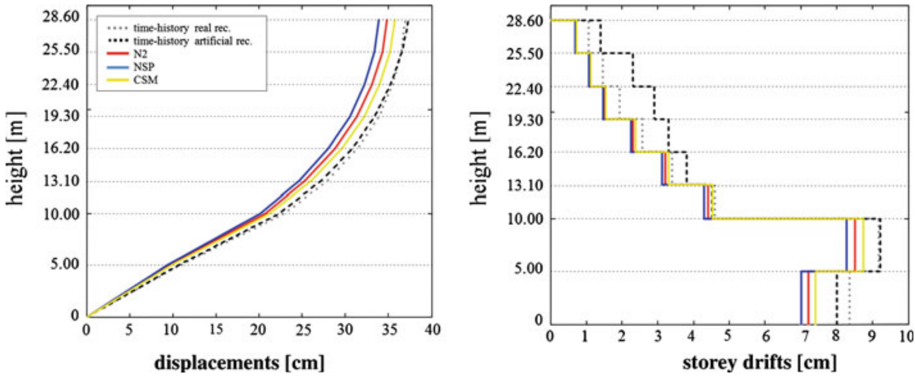


**Fig. 18** Displacements and storey drifts obtained by non-linear dynamic and static methods

displacements in all methods are given in Table 4. It can be noted that the values are similar and correspond to the mean value obtained by non-linear time-history analysis.

Taking into consideration that all the methods use the same pushover curve, there is not much difference observed in displacements and storey drifts when using different non-linear static procedures, Fig. 18. It is obvious that the non-linear static methods provide very good results in estimating the displacements in comparison to the results of the "accurate" non-linear analysis (the differences are within 10%). Less accurate results are obtained in estimating the story drifts, especially on higher storeys, Fig. 18, due to higher mode effects which are not included in the simplified procedures.

It is also advisable to obtain the structure performance in extreme load, which is obtained by increasing the target displacement. There is a recommendation in Eurocode 8/1 that "the capacity curve should be determined by pushover analysis for values of the control displacement ranging between zero and the value corresponding to 150% of the target displacement".

In Table 5 the results of the analysis of the structure from Fig. 1 with control displacement of 150% of the target displacement are presented for all non-linear static methods. Maximum top displacement of the structure in Fig. 1 obtained by using a dynamic method with real time-history records (Fig. 18) is 37.8 cm, which corresponds to 145% of the target displacement obtained using the non-linear static N2 method, Fig. 9.

Increasing the target displacement obtained using the N2 method by a factor of 1.45 equals the maximum displacement of the top of building as if it were obtained by non-linear time-history analysis.

Although it is recommended in EC8/1 to construct the capacity curve taking into account 150% of the target displacement it does not mean the capacity curve should be always idealized based on this value. In Annex B of EC8/1 the iterative procedure is recommended when the supposed and evaluated maximum displacement are very different (see B.5 of EC8/1). For each iterative procedure the elastic-plastic relationship from Fig. 9 will be slightly changed and adopted to the new value of the target displacement according to relation (B.6), EC8/1.

**Table 5** Values of 150% of target displacement for different non-linear static methods and results of non-linear time-history analysis

| | | |
|---|---|---|
| N2 | | |
| Target displacement | 26.1 cm | |
| 150% of target displacement | 39.2 cm | |
| NSP* | | |
| Target displacement | 25.4 cm | |
| 150% of target displacement | 38.1 cm | |
| CSM | | |
| Target displacement | 26.8 cm | |
| 150% of target displacement | 40.2 cm | |
| Time-history | Real | Artificial |
| Minimal value ($\delta_{min}$) | 19.7 cm | 25.5 cm |
| Maximal value ($\delta_{max}$) | 37.8 cm | 29.9 cm |
| The difference $\delta_{max} - \delta_{min}$ | 18.1 cm | 4.4 cm |
| Mean value ($\delta_{AV}$) | 27.7 cm | 28.0 cm |
| Standard deviation ($\sigma$) | 6.8 cm | 0.6 cm |
| Mean value+1$\sigma$ ($\delta_{AV} + \sigma$) | 34.5 cm | 28.6 cm |

In the analysis presented here the iterative procedure has not be carried out (the change of the result of the iterative procedure is negligible).

By increasing the target displacement obtained using the N2 method by a factor of 1.32 the mean value enlarged with the standard deviation obtained by non-linear time-history analysis will be reached, $(\delta_{AV} + \sigma) = 34.5$ cm, Table 5.

In Fig. 18 the results for displacement shapes and storey drifts obtained by non-linear time-history analysis and non-linear static methods based on European and US provisions are presented. The comparison of results obtained by different methods can be seen in Table 5.

Despite the stated insufficiencies non-linear static methods can be a valuable tool in estimating the seismic structural performance for structures in which the influence of the higher modes is not important.

## 8 Conclusions

It can be concluded that the discussed non-linear static methods differ in their application, simplicity, transparency and clarity of theoretical basis, but the basis of all methods is the same, i. e., the pushover method. The main difference among the presented methods is the determination of the pushover limit of target displacement. Three different displacement forms (uniform, triangular and modal) were applied and the differences of the obtained target displacement have been presented.

According to the results of the analysis presented here, the N2 method and the NSP coefficient method are essentially very similar and provide the same results if the starting assumptions are identical. In the NSP coefficient method there are two additional coefficients which influence the value of the target displacement and which are not included in the other two methods (N2 and CSM). Neither of the analyzed methods takes into consideration the accumulation of the damage which can be significant for long duration earthquakes. The inclusion of this effect into the existing methods can be made by increasing the seismic demand or by introducing the equivalent ductility factor like in the N2 method, which reduces the deformation capacity.

Bearing in mind that the non-linear time history analysis is the most accurate method, its results were used for evaluating other methods. The maximum target displacements in all methods are obtained. The values for non-linear static analysis are similar and correspond to the mean value obtained by non-linear time-history analysis.

The structural performance at extreme load, which is obtained by increasing the target displacement, has also been discussed. Maximum top displacement of the structure obtained by using a dynamic method with real time-history records (envelope) corresponds to 145% of the target displacement obtained using the non-linear static N2 method. It means that increasing the target displacement obtained using the N2 method with a factor of 1.45 equals the maximum (envelope) displacement of the top of building as if it were obtained by a non-linear time-history analysis. By increasing the target displacement obtained using the N2 method with a factor of 1.30, the mean value enlarged with the standard deviation obtained by non-linear time-history analysis is reached.

**Acknowledgments** The research in this paper was done within the research project "Development of structures with increased reliability with regard to earthquakes" supported by the Ministry of Science, Education and Sports of the Republic of Croatia (grant no. 114-0821466-1470).

## References

Applied Technology Council (ATC-40) (1996) Seismic Evaluation and Retrofit of Concrete Buildings, Washington, DC

Causevic M, Zehentner E (2007) Non-linear seismic analysis of structures according to EN 1998-1:2004, Gradevinar, Zagreb, No. 09

Chopra AK (2001) Dynamics of structures—theory and applications to earthquake engineering. 2nd edn. Prentice Hall, New Jersey

Chopra AK, Goel RK (1999) Capacity-demand-diagram methods for estimating seismic deformation of inelastic structures. Pacific Earthquake Engineering Research Centre

Chopra AK, Goel RK (2002) A modal pushover procedure to estimate seismic demands of buildings. Earthq Eng Struct Dyn 31:561–582

Eurocode 8 (2004) Design of structures for earthquake resistance, Part 1: General rules, seismic actions and rules for buildings, European standard EN 1998-1. European Committee for Standardization (CEN), Brussels

Fajfar P (2000) A nonlinear analysis method for performance based seismic design. Earthq Spectra 16(3):573–592

Fajfar P, Gaspersic P (1996) The N2 method for the seismic damage analysis of RC buildings. Earthq Eng Struct Dyn 25:23–67

Federal Emergency Management Agency (FEMA) (2005) Improvement of Nonlinear Static Seismic Analysis Procedures—FEMA-440. Washington, DC

Federal Emergency Management Agency (FEMA) (1997) NEHRP guidelines for seismic rehabilitation of buildings—FEMA 273; NEHRP Commentary on the guidelines for the seismic rehabilitation of buildings—FEMA 274. Washington, DC

Federal Emergency Management Agency (FEMA) (2000) Pre standard and Commentary for the Seismic Rehabilitation of Buildings—FEMA 356. Washington, DC

Gelfi P (2007) SIMQKE_GR, Programma per la generazione di accelerogrammi artificiali spettro-compatibili. University of Brescia, Italy

Mitrovic S, Causevic M (2009) Non-linear static seismic analysis of structures, Gradevinar, Zagreb, No. 6

Naumoski N (1988) Representative ensembles of strong earthquake records, CAEE—The Canadian Association for Earthquake Engineering, http://www.caee.uottawa.ca/

Naumoski N, Tso WK, Heidebrecht AC (1988) A selection of representative strong motion earthquake records having different A/V ratios. Earthquake Engineering Research Group, McMaster University, Hamilton, ON, EERG Report 88-01

NISEE—National Information Service for Earthquake Engineering— University of California Berkeley, Earthquake Engineering Research Centre, http://nisee.berkeley.edu

Pinho R, SeismoSoft SeismoSignal (2007) A computer program for processing strong-motion data, URL:http://www.seismosoft.com

Pinho R, SeismoSoft SeismoStruct (2007) A computer program for static and dynamic nonlinear analysis of framed structures, URL:http://www.seismosoft.com

Rozman M, Fajfar P (2009) Seismic response of a RC frame building designed according to old and modern practices. Bull Earthq Eng 7(3):779–799